FINITE ELEMENT ANALYSIS OF EARTH PRESSURES FOR NARROW RETAINING WALLS

Kuo-Hsin Yang[1] and Chia-Nan Liu[2]

ABSTRACT

High traffic demands have led to widening of existing highways to accommodate increased traffic volume. However, due to the high cost of additional right-of-way and limited space available at job sites, construction of earth retaining walls is often done under a constrained space. This leads to retaining walls that are narrower than in design guidelines. This type of walls is referred as "Narrow" retaining walls. Various studies suggest the mechanics of narrow retaining walls differs from traditional walls and the lateral earth pressures in narrow retaining walls are no longer properly predicated by using conventional at-rest or active equations. This paper presents finite element analyses of earth pressures in narrow retaining walls for both at-rest and active conditions. The predicted data show a favorable agreement with measured data from centrifuge tests. The results indicate that, due to arching effects and boundary constraint, the earth pressures decrease as the decrease of the wall aspect ratio for both at-rest and active conditions. The results imply that earth pressure theories would overestimate the earth pressures and the design guideline based on the values of conventional earth pressure is somewhat overly conservative and uneconomical when applying to the design of narrow walls. A new design method especially for narrow wall is proposed by modifying the earth pressures in FHWA MSE wall design guidelines.

Key words: Narrow retaining wall, earth pressure, arching effect, boundary constraint.

1. INTRODUCTION

As the population increases and development of urban areas becomes a priority, the traffic demands have increased which has led to widening of existing highways to accommodate increased traffic volume. One solution is to build mechanical stabilized earth (MSE) walls in front of previously stabilized walls. The acceptance of MSE walls has been driven by a number of factors, including aesthetics, reliability, cost, construction techniques, seismic performance, and the ability to tolerate large deformations without structural distress. However, due to the high cost of additional right-of-way and limited space available at job sites, construction of earth retaining walls is often done under a constrained space. This leads to retaining walls that are narrower than in current design guidelines. An example of "Narrow" retaining walls is illustrated in Fig. 1.

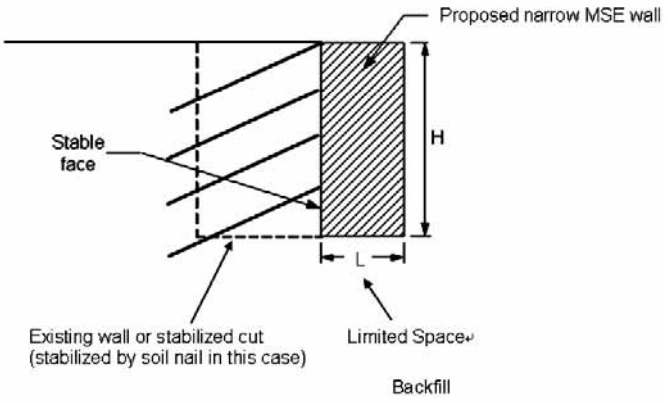

Fig. 1 Illustration of proposed narrow MSE wall in front of a stable face

This paper presents a study to investigate the design of narrow retaining walls in front of stable faces. The motivation for the research is twofold. First, the construction of narrow retaining walls is not addressed in FHWA guidelines (Elias *et al*., 2001). The existing state-of-practice suggests a minimum wall width and MSE reinforcement length equal to 70 percent of the wall height. Second, the design methodology to construct narrow earth retaining structures in front of a stable slope or wall is unclear at present; the design methodology of internal stability in FHWA guidelines is based on: (1) theoretical earth pressure equations (Jacky's equation for at-rest condition or Rankine's equation for active condition) to calculate the factor of safety against breakage and; (2) the assumption of linear failure surface to calculate the factor of safety against pullout. However, those are not the cases for narrow walls. Various studies (*e.g.*, Spangler and Handy, 1984; Leshchinsky *et al*., 2003; Lawson and Yee, 2005; Frydman and Keissar, 1987; Take and Valsangkar, 2001; Woodruff, 2003) suggested the earth pressure would be less than theoretical earth pressure. In addition, based on centrifuge test results (Woodruff, 2003), the failure surface would become bilinear instead of linear because of the limitation of space for fully developing the failure surface. Besides the issues of internal stability, the external stability for narrow walls may be also required different consideration from that for conventional walls. In this paper, the authors focus on the modification of earth pressure in the narrow walls to account for the calculation of the factor of safety against breakage for internal stability.

As aforementioned, the mechanics of narrow retaining walls

Manuscript received March 19, 2007; revised July 5, 2007; accepted July 10, 2007.

[1] Graduate student, Department of Civil, Architectural and Environmental Engineering, The University of Texas at Austin, U.S.A. (e-mail: khyang@mail.utexas.edu)

[2] Associate Professor (corresponding author), Department of Civil Engineering, National Chi Nan University, Taiwan, 545, R.O.C. (e-mail: cnliu@ncnu.edu.tw)

is different from traditional walls and the earth pressures are different from conventional earth pressures. The pressure is affected by the wall geometry and the pressure from the preexisting wall. In this paper, the preexisting wall is assumed to be in a perfectly stable status, that is, there is no pressure acting from the existing wall to narrow retaining wall. For example, the wall reinforced by soil nails as shown in Fig. 1 is assumed as a perfect stable face. The wall geometry in terms of wall aspect ratio, L/H, (wall width, L, over wall height, H) is the only factor considered in this study affecting the distribution and magnitude of earth pressure behind the newly constructed narrow MSE wall. The effect of pressure from an existing wall acting on narrow retaining walls can be addressed in future study.

The effect of varying the wall widths of retaining wall on earth pressure through has been conducted by several researchers through using the methods of the differential equation (*e.g.*, Spangler and Handy, 1984), limit equilibrium analyses (*e.g.*, Leshchinsky *et al*., 2003; Lawson and Yee, 2005) and centrifuge tests (*e.g.*, Frydman and Keissar, 1987; Take and Valsangkar, 2001; Woodruff, 2003). However, finite element analysis has never been applied in this topic. The objective of this research is to explore the earth pressure behind narrow walls by using finite element analysis. First, the numerical model and the parameters of soil constitutive model in this study are introduced. Then, the model is verified by the data from centrifuge tests collected from published literatures. A series of parametric studies is performed to investigate the effect of wall aspect ratios on the earth pressures in both at-rest and active conditions. Two charts of the calculated earth pressure versus wall aspect ratio are provided for the basis of further application and design of narrow wall. The charts for at-rest case could be applied to rigid retaining walls or MSE walls with inextensible reinforcements; and the chart for active case could be applied to flexible retaining walls or MSE walls with extensible reinforcements. Finally, a new design method especially for narrow wall condition is proposed by modifying from FHWA MSE wall design guidelines.

2. BACKGROUND

The study of earth pressure started from Rankine for active earth pressure in 1860 and from Jaky for at-rest earth pressure in 1944. Their calculated earth pressures were only applicable to the case of backfill with unlimited space. The study of pressure in a constrained space originated from the agriculture to investigate the pressure of silos filled with grain or corn (*e.g.*, Blight, 1986; Jarrett *et al*, 1995). Janssen (Janssen, 1895; translation and comment by Sperl, 2006) proposed the arching theory to describe the reduction of pressures. The reduction of pressures is known as arching effect. Arching effect is the result of an interaction between wall-soil interfaces. As soil is placed, soil layers settle due to its self weight and the load applied by additional soil layers above. Simultaneously, the wall will provide a vertical shear load due to friction that resist the settlement of soil. The vertical shear load reduces the soil overburden pressure and, consequently, reduces the lateral earth pressure (*e.g.*, Handy, 1985; Filz and Duncan, 1997a, 1997b).

From a geotechnical perspective, Spangler and Handy (1984) proposed the following arching equation, based on Janssen's theory, to calculate the lateral earth pressure coefficient at a specific level in the fill:

$$k = \frac{1}{2\tan\delta} \cdot \frac{L}{z} \cdot \left[1 - e^{-2 \cdot K \cdot \frac{z}{L} \cdot \tan\delta} \right] \quad (1)$$

where

L is the backfill width;

z is the backfill depth;

δ is the soil-structure interface friction angle;

K is the conventional earth pressure coefficient;

for at-rest condition, use Jaky's earth pressure coefficient, $K_o = 1 - \sin\phi'$;

for active condition, use Rankine's earth pressure coefficient, $K_a = \tan^2(45° - \phi'/2)$;

Equation (1) is referred to as the arching equation henceforth and, later on, will be used to compare with the earth pressures from centrifuge tests and finite element simulation.

Frydman and Keissar (1987) conducted a series of centrifuge tests to investigate the earth pressure on retaining walls near rock faces in both the at-rest and active conditions. The aspect ratio of the soil behind the wall was varied among tests from 0.1 to 1.1. They found that the measured earth pressure decreased from conventional at-rest values for at-rest condition or from conventional active values for active condition as the depth increased below the surface. Frydman and Keissar compared their test to arching equation, Eq. (1), and concluded that arching equation has a good prediction in at-rest condition but an underestimation in active condition. Take and Valsangkar (2001) also performed a series of centrifuge tests to study the earth pressure on unyielding retaining walls of narrow backfill width. The wall aspect ratios ranged from 0.1 to 0.7. Their test agreed with Frydman's finding. Woodruff (2003) performed a comprehensive series of centrifuge model tests on reinforced soil walls adjacent to a stable face. Woodruff tested 24 different walls with reinforcement lengths (wall widths) ranging from 0.17 to 0.9 times the wall height. He observed that when the wall aspect ratio decreased, the failure mode transformed from internal failure (breakage of reinforcement) to external failure (overturning). By authors' interpretation, this fact implied that the earth pressure decreased with the decrease of the wall aspect ratio so that the internal failure was not the major failure mode in low wall aspect ratio.

Leshchinsky *et al*. (2003) performed a series of limit equilibrium analyses of MSE walls with limited space between the wall and a stable face. They showed that as the aspect ratio decreased, the earth pressure coefficient also decreased, most likely due to the restricted space in which potential slip surfaces could form. Lawson and Yee (2005) used an approach similar to Leshchinsky to develop design charts for the earth pressure coefficients. They considered planar and bilinear slip surfaces, including composite slip surfaces that passed through the reinforced soil as well as along the interface between the reinforced soil and the stable face behind the wall. They showed that the forces were less than those for active earth pressures and decreased as the aspect ratio decreased.

3. NUMERICAL MODEL

The finite element program Plaxis version 8 (Plaxis, 2005) was used to conduct the numerical analysis in this study. Figure 2

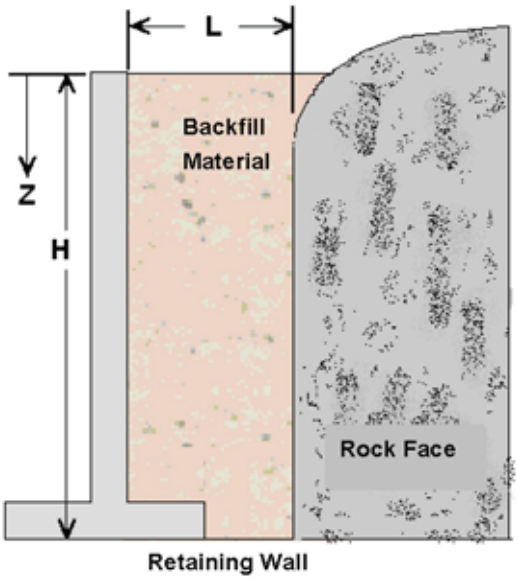

Fig. 2 Illustration of the simulated case

illustrates the case of narrow retaining walls in front of a stable rock face. Figure 3(a) is the finite element model simulating this case in Fig. 2 for at-rest condition. Figure 3(b) is the finite element model for active condition. In Fig. 3(a), a horizontal fixity is superposed on facial structure to prevent it from horizontal movement. The horizontal fixity guarantees the wall keeping in at-rest condition. In Fig. 3(b), a prescribed displacement is added to rotate the wall facing structure outward and force the backfill in the wall to reach failure stage to simulate active condition. Wall aspect ratios were varied by changing model widths.

The finite element meshes are composed of 15-node isoparametric triangular elements to model the soil. This 15-node triangle is considered a very accurate element that has produced high quality stress results for difficult problems. The mesh coarseness was set as "Fine", which would generate around 500 triangular elements for a given geometry. The procedure of stage construction was also included by conducting layer-by-layer construction in Plaxis; totally ten construction layers were evenly divided through out the wall height. Mohr-Coulomb model was chosen as the soil constitutive model. Total fixities were used to represent the stable face. Plate elements were used to represent the facial structure of retaining wall. Plates are structural objects composed of beam elements with bending stiffness, *EI*, and a normal stiffness, *EA*. In this study, the deformation of the plate was out of interest so the bending and normal stiffness of the plate were set high enough to prohibit the compression and bend occurring in the plate.

In order to simulate the earth pressures developed between new constructed wall face and preexisted stable wall, interface elements were employed at both front and back sides of backfill zone to capture the interaction between backfill soil and wall face structure. An elastic-plastic model was used to depict the behavior of interfaces. The Mohr-Coulomb criterion was used to distinguish between elastic behavior and plastic interface behavior when permanent slip may occur. Plane strain analysis was implemented as a benefit of solving the three-dimensional problem by using two-dimensional analysis. Compaction stresses induced during construction was not accounted for in the analysis.

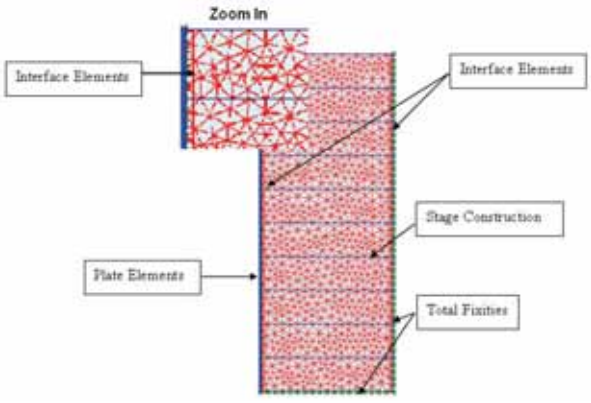

Fig. 3(a) Finite element meshes for at-rest case

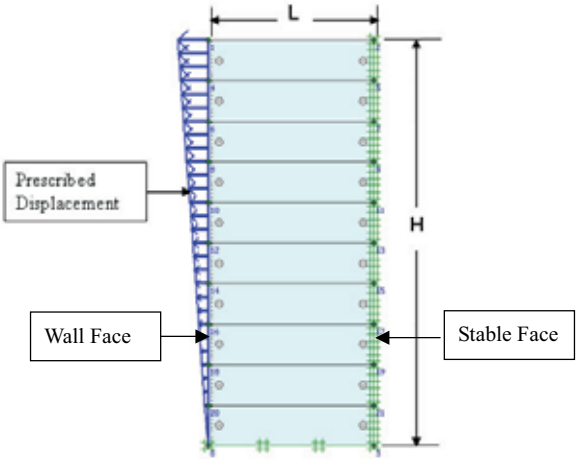

Fig. 3(b) Finite element model for active case

4. NUMERICAL ANALYSIS RESULTS AND VERIFICATION

The literature review showed that the arching effect (interface interaction) and boundary constraint (varying of wall widths) were the two main factors influencing earth pressures in narrow retaining walls. The proposed finite element model was conducted to study these effects by modeling two sets of centrifuge tests reported on literature. First, Frydman's centrifuge tests results (Frydman and Keissar, 1987) were numerically modeled to investigate the effect of interface interaction on the calculated earth pressures for at-rest and active conditions. The target was to check the arching effect in finite element model. Second, Take's centrifuge tests (Take and Valsangkar, 2001) were modeled to study the sensitivity of calculated earth pressures with varying wall aspect ratios to look into the effect of boundary constraint.

4.1 Verifying the Arching Effect

Frydman conducted a series of centrifuge tests to investigate the earth pressure on retaining walls near rock faces in both at-rest and active conditions. Tests were run on models with ratios of L/H = 1.1, 0.3, 0.22, 0.19, and 0.1. The models were built in an aluminum box and each model included a retaining wall made

from aluminum (195 mm high × 100 mm wide × 20 mm thick) connected to the base of the box. The rock face was modeled by a wooden block coated with the backfill material, so that the friction between the rock face and the backfill was essentially equal to the angle of internal friction of the backfill. The granular fill between the wall and the rock face was modeled using Haifa Bay uniform fine sand. Particle size was in the range of 0.1 ~ 0.3 mm, density between 14.0 ~ 16.4 kN/m^3 and the sand was placed at a relative density of 70%. Direct shear tests performed on the sand at this relative density gave values of the angle of internal friction, ϕ', equal to 36°. Direct shear test between the sand and aluminum yielded values of the angles of interface friction, δ, between 20° ~ 25°. Load cells (Kyowa, LM-A series) were inset flush with the wall face near the top and bottom of the wall. The model was spun up to 43.7 g without any wall movement. Load cell readings at this stage yielded values of at-rest pressure. The wall was then allowed to rotate about its base. Load cell readings at this stage yielded values of active pressure. The stress levels developed in these models would be similar to those next to full scale walls having a height of about 8.5 m.

Finite element analyses were performed using the previously mentioned wall geometries and backfill properties. The Mohr-Coulomb model was used as a soil constitutive model for the sake of simplicity and the lack of stress-strain curves which were necessary for a more sophisticated constitutive model like Duncan hyperbolic model. Young's modulus, E, and Poisson's ratio, ν are not specified in Frydman's paper; however, the at-rest earth pressure is well known as a function of Poisson's ratio. PLAXIS manual suggests using following approach to determine realistic Poisson's ratio. Authors inputted a value of Poisson's ratio that will give the K_o matching the K_o calculated from input frictional angle. In other words, the input Poisson's ratio should satisfy the following criterion:

$$K_o = 1 - \sin\phi = \frac{\nu}{1-\nu} \tag{2}$$

Young's modulus has only little influence on predicted earth pressures and an average value of Young's modulus of sand is assigned for this simulation. Table 1 provides model parameters for simulating Frydman's tests. For avoiding the difficulty of numerical calculation, a small cohesion value (C = 1 kPa) was introduced in the soil model to prevent premature soil yielding in locally low confining pressure zones. This value was selected to be as small as possible to keep the input soil strength close to measured strength from triaxial tests. The approach of introducing a small cohesion value was also suggested by Hatami and Bathurst (2005).

The lateral earth pressure coefficients from tests, arching equation and finite element simulation are showed in Fig. 4(a) for at-rest condition and in Fig. 4(b) for active condition. The depth is presented as the non-dimensional quantity z/L where z is the depth below the top of wall and L is the wall width. Similarly, the lateral earth pressure along the wall face is represented by the non-dimensional lateral earth pressure coefficient k_w'. In Fig. 4(a), because of apparent arching effects, the earth pressure coefficients start at K_o near the top of the wall and decrease with depth below the top of the wall. Except for the divergence at $z/L < 0.5$, the results of measurements, arching equation and the finite element simulation agree favorably well. The discrepancy between

Table 1 Model parameters for simulating centrifuge tests

Symbols	Values		Unit
	Frydman's tests	Take's tests	
Unit weight, γ	16.4	16.2	kN/m^3
Frictional angle, ϕ'	36	36	deg.
Cohesion, C	1	1	kN/m^2
Young's modulus, E	30,000	30,000	kN/m^2
Poisson's ratio, ν	0.3	0.3	
Interface strength, R_{inter}	2/3	2/3	

[a] Cohesion was set a small value for numerical purpose
[b] R_{inter} = tan δ / tan ϕ'

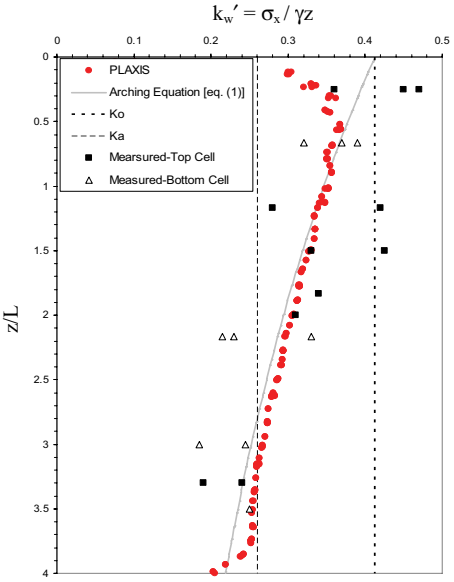

Fig. 4(a) Finite element simulating Frydman's centrifuge test for at-rest case

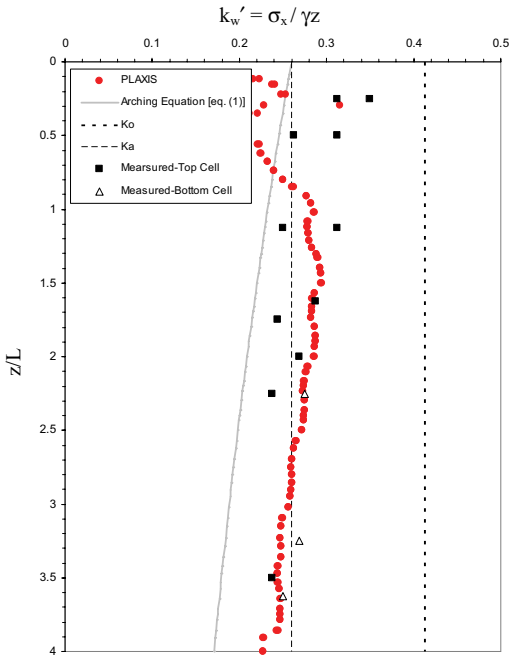

Fig. 4(b) Finite element simulating Frydman's centrifuge test for active case

measured results and finite element simulation for $z/L < 0.5$ are due to low overburden pressure at the top of the wall.

In Fig. 4(b), finite element simulation is still in a good agreement with measurement; however, arching equation considerably underestimates the values. It is observed from the FEM analysis results that the values of the finite element simulation are around K_a and don't have notable decrease with the depth. This evidence suggests that arching effect is less obvious for active condition due to the movement of the wall face attenuating the effect of soil-structure interaction. This observation is consistent with the explanation provided by Frydman. He stated that the underestimation was attributed to the progressive failure in the sand adjacent to the rotation wall. Sand was loosened and the density around that area was lower than that before the wall was rotated. Consequently, the frictional angle decreased as the decrease of density and lower values of frictional angle should be adjusted to arching equation.

4.2 Verifying the Effect of Boundary Constraint

Take carried out a series of centrifuge tests to investigate the earth pressures on unyielding retaining walls with narrow backfill widths. All model walls were 140 mm high but had various widths corresponding to the wall aspect ratios ranged from 0.1 to 0.7. The model backfill material was classified as poorly graded sand with little or no fines. The backfill material had mean particle size of 0.4 mm, minimum and maximum dry densities 13.4 and 16.2 kN/m^3, respectively, and a relative density of 79%. A series of direct shear tests was performed to obtain the angle of internal friction $\phi' = 36°$, and the interface friction angles with an aluminum wall face, $\delta = 23° \sim 25°$. Six boundary pressure cells were housed and distributed evenly over the height of the model fascia retaining wall. All centrifuge retaining wall experiments were performed at an acceleration of 35.7 g to simulate a 5 m high prototype wall.

Two finite element analyses were performed for wall widths equal to 15 mm and 75 mm, namely, corresponding to the Test D and Test B, $\delta_{wall} = \delta_{rock}$ in Take's tests. Model parameters for simulating Take's test were also listed in Table 1.

Figure 5 shows the results from tests, arching equation and the finite element simulation for two different wall widths to inspect the effect of boundary constraint on calculated earth pressures. The results are presented as depth versus horizontal stresses. The decrease of earth pressures becomes prominent as the width of the wall becomes less (boundary constraint increases). The reason accounting for boundary constraint induced decrease of earth pressures is similar to the case of plane strain. The reduction of freedom for movement would increase soil strength in terms of frictional angle and, consequently, reduce earth pressures.

4.3 Summary and Commentary

It has been demonstrated that, for at-rest condition, both finite element simulation and arching equation can predict well the earth pressures measured from centrifuge tests; however, for active condition, finite element simulation shows better match to centrifuge tests than arching equation.

According to Leshchinsky *et al*. (2003), the decrease of earth pressures with the decrease of wall aspect ratio occurs due to the absence of full development of potential slip surfaces in the restricted space during active condition. But the authors

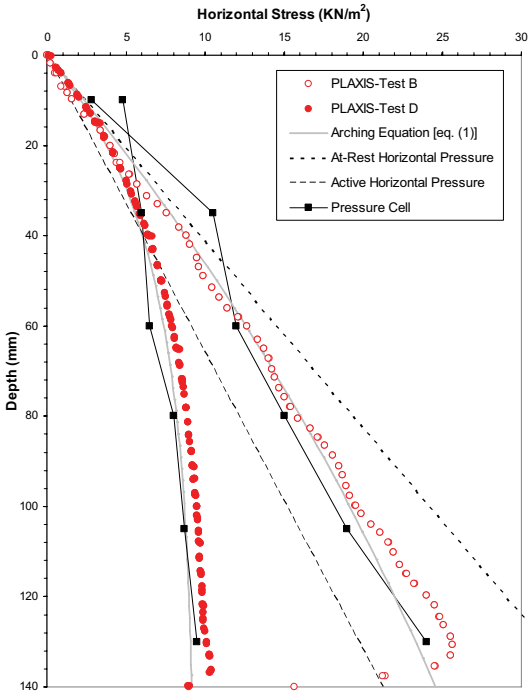

Fig. 5 Finite element simulating Take's centrifuge test

observed decrease in earth pressure even for at-rest condition where no slip surface was formed. It is believed that the possible reason for this is arching effect and boundary constraint as explained previously.

In conclusion, the promising results prove that the finite element analysis can accurately capture the behavior of retaining wall responding to arching effect and boundary constraint for both at-rest and active conditions. The verification with laboratory test results also provides justification of applying the proposed finite element model for further parametric study and applications.

5. PARAMETRIC STUDY

5.1 Effect of Varying Wall Aspect Ratio

A series of parametric study was conducted to explore the effect of varying wall aspect ratios on the earth pressures. The wall height was fixed to 10 m while wall width corresponding to desired wall aspect ratios (L/H = 0.1, 0.3, 0.5, 0.7) was set during parametric study. Predicted earth pressure coefficients were normalized by K_a. Two vertical earth pressure profiles were of interest: one is along the wall face and the other is along the center of the wall (a vertical plane midway between the face of the wall and back of the backfill). Note that not all of the horizontal stresses output from all stress points were exhibited. Instead, data points were averaged at each 0.1 z/H interval for the ease of observing the variation of trends.

Normalized earth pressure coefficient profiles for at-rest condition are shown in Figs. 6(a) and 6(b). The symbol k_w' denotes the calculated earth pressure coefficients along the wall face and k_c' represents the calculated earth pressure coefficients along the center of the wall. Beside the discrepancy at $z/H < 0.15$ in Fig. 6(a), the earth pressures decrease with depth and with

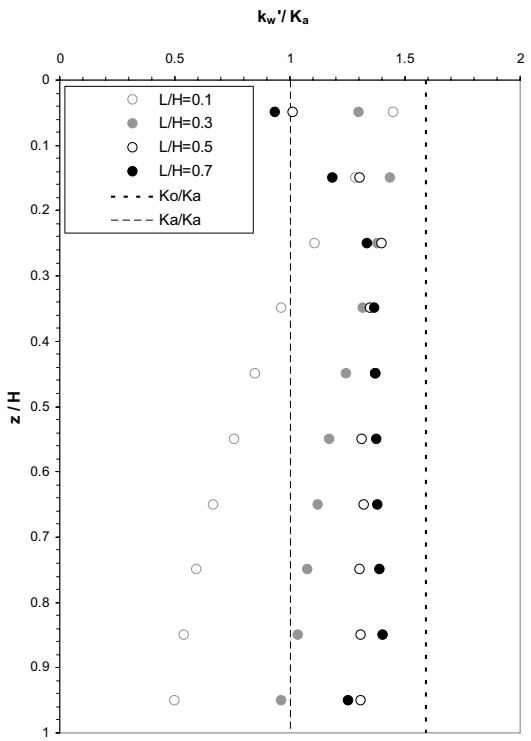

Fig. 6(a) Normalized earth pressure coefficient profiles along the wall face for at-rest case

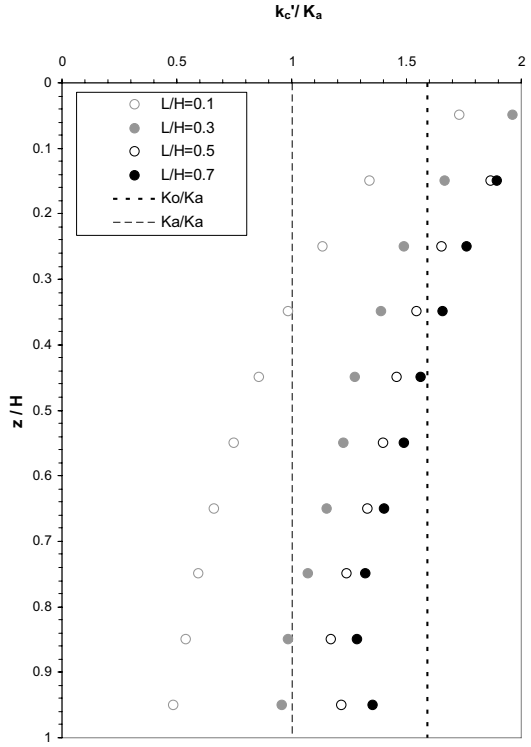

Fig. 6(b) Normalized earth pressure coefficient profiles along center of the wall for at-rest case

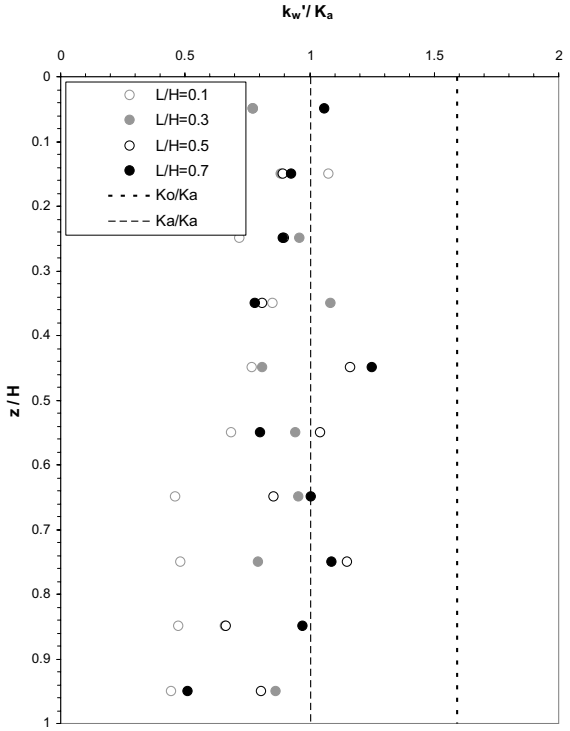

Fig. 7(a) Normalized earth pressure coefficient profiles along the wall face for active case

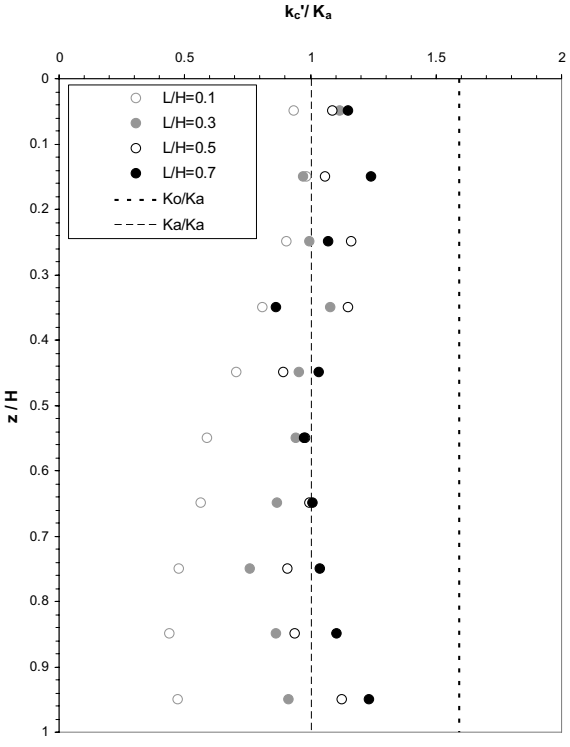

Fig. 7(b) Normalized earth pressure coefficient profiles along center of the wall for active case

decreasing aspect ratios in both figures. The active (K_a/ K_a) and at-rest (K_o/K_a) earth pressure coefficients are also plotted for reference.

Normalized earth pressure coefficient profiles for active condition are addressed in Figs. 7(a) and 7(b). First, the data are scattered around K_a and don't show a clear tendency to decrease the earth pressures with depth below the surface; the progressive failure in the soil mass attenuating the arching effect can be accused as the cause. Even so, we still can see earth pressure profiles decrease (shift to the left side of figures) as the decrease of aspect ratio. The effect of boundary constraint still can be recognized that it decreases earth pressures for active condition.

5.2 Charts of the Equivalent Earth Pressure *vs.* Wall Aspect Ratio

The parametric analysis results are prepared as normalized equivalent earth pressure coefficients *vs.* wall aspect ratio, as shown in Fig. 8 for at-rest case and Fig. 9 for active condition, to simplify the observation of parameter effects and for an easy application. Capital "*K*" representing the equivalent earth pressure coefficient is used to distinguish from little case "*k*" which means the earth pressure coefficient at a specific level. The equivalent earth pressure is a simple indicator which captures the complexity of simulation and is an appropriate indicator of the stress distribution. The calculated equivalent earth pressure is defined below:

$$K' = \frac{\int_0^H k'\gamma\, z\, dz}{\frac{1}{2}\gamma H^2} \tag{3}$$

where

H is the wall height;

k' is the calculated earth pressure coefficient;

z is the backfill depth;

γ is the soil unit weight.

Figure 8 is for at-rest case showing the equivalent earth pressure coefficients along the wall face, K_w', along the center of the wall, K_c', and the equivalent earth pressure coefficients computed from arching equation. All the pressure coefficients are normalized by K_a. Several points are important and discussed as follows. First, the data from finite element analyses clearly show the normalized equivalent earth pressure coefficients are less than K_o/K_a by 10% to 60% when the aspect ratio changed from 0.7 to 0.1. The difference from K_o/K_a is most likely due to some arching effects and boundary constraint. Even when the wall aspect ratio equal to 0.7, which the state-of-practice suggests as a minimum values, the equivalent earth pressure along the center of the wall is still around 10% less than K_o. Filz and Duncan (1997a) proposed a theory to compute the reduction of lateral earth pressures due to the vertical shear loads on an unyielding wall. They found the lateral earth pressure is 8% less than K_o for soil frictional angle $\phi' = 35$. Their result, 8%, is close to the 10% in the presented study. Second, the computed equivalent earth pressures using arching equation are slightly less than the predicted equivalent earth pressures using finite element method. The difference is probably due to difference in boundary condition at the bottom of the wall. In the finite element analyses, boundary was fixed at bottom; however, no boundary at bottom was considered in arching equation. The fix boundary at bottom of wall would increase soil stress locally around bottom and increase the equivalent earth pressure slightly. This fact could be observed in Figs. 4(a) and 5. Third, the earth pressures along the wall face are compared to that at the center of the wall. At same wall aspect ratio, earth pressures along the center of the wall are higher than that along the wall face. This is because soil and structure have a more intensive interaction along the wall face and this vigorous interaction would decrease the earth pressures along the wall face.

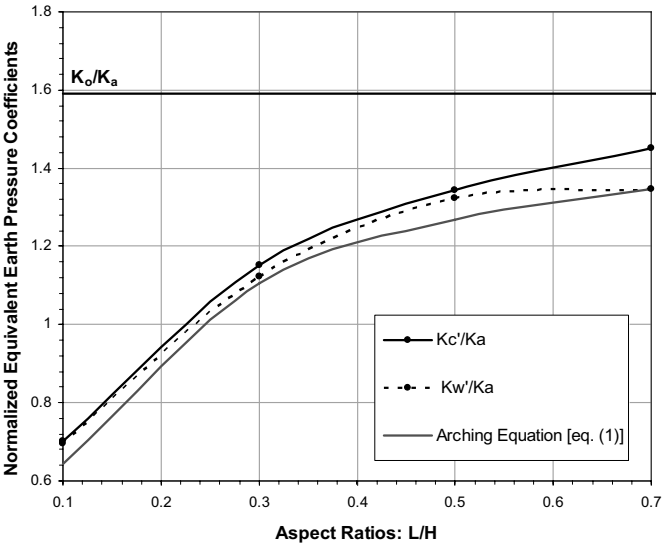

Fig. 8 Normalized equivalent earth pressure coefficients for at-rest case

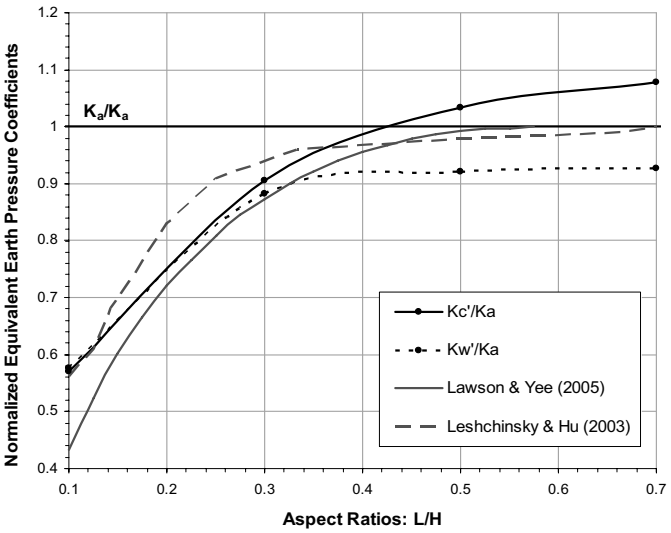

Fig. 9 Normalized equivalent earth pressure coefficients for active case

Figure 9 is for active case. All the pressure coefficients are normalized by K_a. Several points are discussed as follows. First, the decreasing tendency of equivalent earth pressure from finite element analyses is not obvious until $L/H < 0.3$. This implies that the boundary constraint starts to play role when the shape of wall becomes very slender. Second, K_c' / K_a is larger than one at $L/H = 0.7$. This may be because the failure wedge which inclines at $(45° + \phi'/2)$ from horizon extends at the front toe of the wall and the stress points (used to calculate equivalent earth pressures) around bottom middle part of wall are not involved inside the failure wedge. The stress points outside the failure wedge would cause the corresponding earth pressure coefficients greater than K_a and, therefore, the equivalent earth pressure coefficient would be greater than K_a. This fact is shown at earth pressure coefficient profile at $L/H = 0.7$ in Fig. 7(b). Third, the earth pressures along the wall face are compared to that along the center of the wall. The difference is apparent and it is most likely because all the stress points along the wall face is inside the failure wedge but

not all of the stress points at the center of the wall is at failure stage. This difference for active condition is larger than that for at-rest condition. This difference is caused by the difference locations of stress points (inside or outside of failure wedge) for active condition is larger than the difference caused by arching effect for at-rest condition. Fourth, data from limit equilibrium analyses by Lawson and Yee (2005) and Leshchinsky *et al*. (2003) are compared with calculated data from finite element simulations. They generally show a similar trend. However, the limit equilibrium analyses are the "average" earth pressures. Limit equilibrium analyses don't have the ability to separate out the different earth pressures at different locations; nevertheless, it is crucial to select the maximum values rather than the average values for practical design.

Although Figs. 8 and 9 were developed based on only single value of soil frictional angle, $\phi' = 36°$, those charts are applicable for a greatly range of soil frictional angles because the friction angle has little effect when the equivalent earth pressures are normalized by K_a, where K_a is also a function of ϕ'. However, engineer should use this chart carefully. The backfill of the narrow MSE wall is usually limited for gravel or sand materials. Figures 8 and 9 are not appropriate for using locally, naturally cohesive materials as backfill because the arching effect in cohesive material has been questionable.

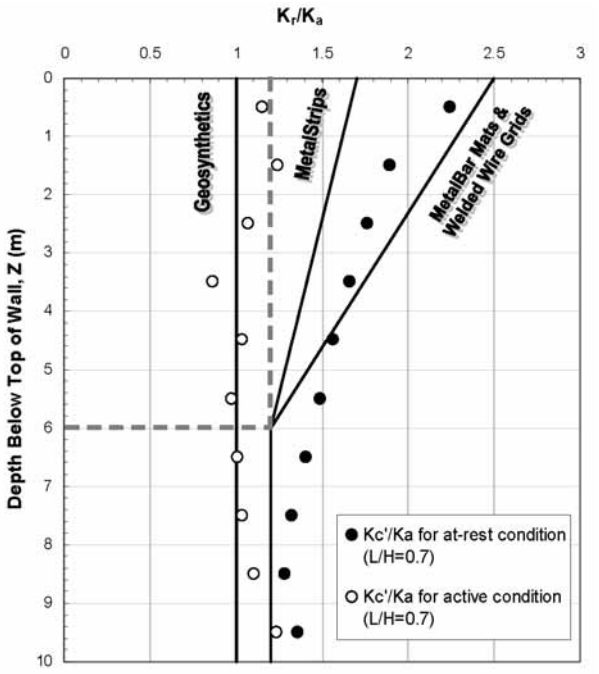

Fig. 10 Comparison of normalized earth pressure coefficient profiles with those in FHWA MSE wall design guidelines

6. APPLICATION

The earth pressures in the FHWA criteria are for MSE walls having unlimited space or $L/H > 0.7$. One observation has been made through this study that the earth pressures would decrease as the decrease of the wall aspect ratios. This observation implies the values of earth pressures provided in design guidelines are somewhat overly conservative and uneconomical when applied to the design of narrow walls where the reduction of earth pressure due to arching effect and boundary constraint prevails. A reconsideration and revision of design guidelines specifically for narrow MSE walls is conducted in this study. The calculated earth pressure profiles are compared to the FHWA design guidelines in Section 6.1. Then, a new design method modified from FHWA design guidelines is described by a practical example in Section 6.2.

6.1 Comparison of Calculated Earth Pressures to Those in FHWA Design Guidelines

The calculated earth pressure coefficient profiles at $L/H = 0.7$ were plotted together with the design earth pressure coefficients according to the FHWA retaining wall design guidelines, as shown in Fig. 10. $L/H = 0.7$ is selected for comparison because the existing state-of-practice suggests a minimum wall width and MSE reinforcement length equal to 0.7 of wall height. These profiles of the earth pressure coefficient profiles along the center of the wall from Fig. 6(b) for at-rest condition and from Fig. 7(b) for active condition are adopted. The earth pressure along the center of the wall is the maximum earth pressures in the case of the at-rest condition and approximately the maximum values in the case of active condition.

Figure 10 shows the numerical analysis results of K_c'/K_a for at-rest condition corresponds well with the guidelines for metal bars, mats and welded wire grids, *i.e.,* very stiff, inextensible reinforcements. On the other side, the K_c'/K_a for active condition corresponds well with the guidelines for geosynthetics, *i.e.,* very flexible, extensible reinforcements. These agreements suggest that the results from finite element simulations for at-rest condition can be applies to rigid retaining walls or MSE walls with inextensible reinforcements and the results from finite element simulations for active condition can be interpreted to flexible retaining walls or MSE walls with extensible reinforcements.

6.2 New Design Method for Narrow Walls

An example for calculating earth pressure profiles of the wall aspect ratios less than 0.7 is demonstrated in this section. Figure 11 schematically shows how to modify the FHWA design guidelines to calculate the earth pressure profile for the wall aspect ratios 0.3 with inextensible reinforcements. The procedure is easy and only requires two steps as follows:

Step 1: Choose the original line according to the type (or stiffness) of reinforcements

In this example, a wall with inextensible reinforcement is going to be built. Therefore an original line (dash line) in FHWA design guidelines for reinforcement of metal bars, mats and welded wire grids is picked.

Step 2: Shift Points A, B, and C to left Points A*, B*, and C* by multiplying the reduction factor, R_d.

Reduction factors are a ratio of the equivalent earth pressures at any $L/H < 0.7$ to the equivalent earth pressure at wall $L/H = 0.7$. Reduction factors can be calculated as the ratio of K_c'/K_a (any $L/H < 0.7$) to K_c'/K_a ($L/H = 0.7$) in Fig. 8 for at-rest case and Fig. 9 for active case. The reduction factors for both at-rest and active cases are shown in Fig. 12.

As shown in Fig. 11, the calculated data (gray dots) from finite element analyses are basically compatible to the modified line (solid line). It proves that the new method can be applied to estimate earth pressure profiles in narrow walls.

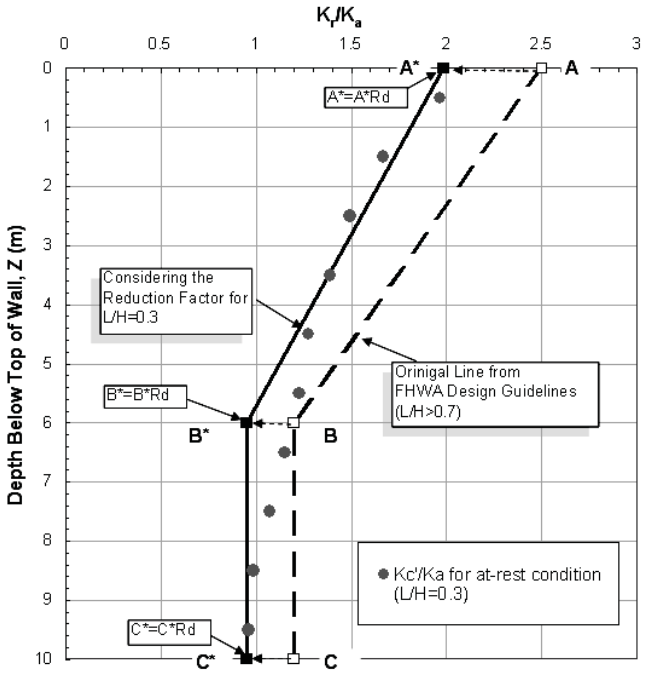

Fig. 11 Scheme showing how to modify FHWA design guidelines for narrow retaining wall

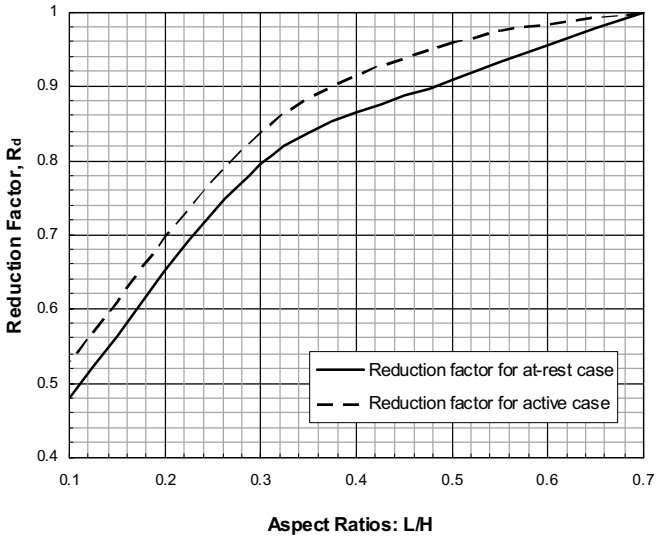

Fig. 12 Reduction factors for various aspect ratios

6.3 Commentary

The new design method allows designers to use "weaker" and "shorter" reinforcements. Because of the lower earth pressure, a use of weaker reinforcement is appropriate in narrow walls. Because of the limited spaces due to the slender shapes of retaining walls, the use of shorter reinforcements is also appropriate. However, it is noteworthy this conclusion is only valid in terms of internal stability. A tall and slender structure is internally safe but not externally. According to the centrifuge tests performed by Woodruff (2003), when wall at $L/H < 0.26$, the failure mode transformed from internal failure (breakage or reinforcement) to external failure (overturning). That is when wall shape becomes extremely slender, the internal stability is no longer important and the external stability of preventing overturning becomes the major issue. Indeed, Lawson and Yee (2005) suggest attaching the reinforcements to anchors or nails inserted into an existing stable wall or stable rock to ensure the external stability and to dissipate the residual tension at the rear of reinforcements. However, this method may rack the stability of existing stable walls and create potential weak interfaces at stable wall faces. Another option is that extend the upper reinforcements over the top of an existing stable wall (see Fig. 13). If the fill is too narrow, cast in place concrete is a good alternative. However, the extra design consideration quantitatively for external stability is required for future work.

7. CONCLUSIONS

In this paper, a series of finite element analysis was performed to investigate the earth pressures behind walls with less than the normal width. The earth pressures at different stages (at-rest or active condition) and at different locations (along the wall face or along the center of the wall) were studied in this paper. This work shows that first, a better capture of arching effect and boundary constraint; and second, the capability of pointing out the values of earth pressures at different locations and different stages, can be achieved by using finite element method. Besides, a new design method for narrow walls has been proposed based on a series of finite element analysis results. The following conclusions were drawn from this study.

(1) The trend of the decrease of earth pressures as the decrease of wall aspect ratios was observed through several literatures as well as finite element analyses in this study. This decreasing tendency could be ascribed to arching effects and boundary constraint. Arching effect was more major in at-rest condition than in active condition in which boundary constraint dominated.

(2) Calculated earth pressures from finite element method were compared to pressures calculated from arching equation, measured values from centrifuge tests, and the pressures calculated using limit equilibrium analyses. Arching equation had a good performance in at-rest condition but an underestimation in active condition. Limit equilibrium analysis is incapable of reporting the earth pressures for at-rest condition and at different locations. Compared with arching equation and limit equilibrium analysis, finite element analysis showed a superior capability.

(3) Based on the parametric study, the design of narrow walls could be somewhat overly conservative and uneconomical by using the design chart in FHWA design guidelines. A new design method tailor-made for retaining walls in narrow spaces was provided based on FHWA design guidelines and the chart of reduction factors.

(4) When $L/H < 0.3$, the failure mode transformed from internal failure to external failure. A quantitatively study for external stability is required for future work.

In the present study, the scope was only focused on the earth pressures of narrow retaining walls in front of an existing wall assumed which was perfectly stabilized (no pressure acting from the existing wall to the narrow retaining wall). In the future study, the effect of pressure from the existing wall should be examined realistically. Besides, the design considerations of preventing the external failure require elaborateness. Moreover, other problems associated seismic loadings, surcharges and the issue of uncertainty analysis should also be incorporated into future study.

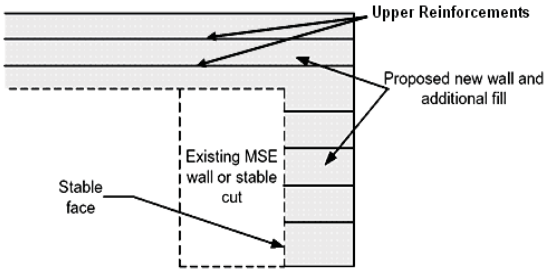

Fig. 13 Extend the upper reinforcements over the top of an existing stable wall

ACKNOWLEDGEMENTS

The work presented herein was supported by Texas Department of Transportation (Project No. 0-5506). The First author is indebted to Dr. Stephen Wright and Dr. Jorge Zornberg from the University of Texas at Austin for their instruction and inspiration and Mr. Ken Kniss for the great discussion and help.

NOTATION

The following symbols are used in this paper

C = cohesion;
E = Young's modulus;
H = wall height;
K = earth pressure coefficient based on Janssen's arching theory in Eq. (1);
k' = calculated earth pressure coefficient; (Note: symbol " ′ " means the value is calculated using the FE model)
k_c' = calculated earth pressure coefficient profile along center of the wall;
k_w' = calculated earth pressure coefficient profile along the wall face;
K = conventional earth pressure coefficient;
K_o = conventional at-rest earth pressure coefficient, $K_o = 1 - \sin\phi'$;
K_a = conventional active (Rankine) earth pressure coefficient, $K_a = \tan^2(45° - \phi'/2)$;
K' = calculated equivalent earth pressure coefficient in Eq. (3);
K_c' = calculated equivalent earth pressure along center of the wall;
K_w' = calculated equivalent earth pressure along the wall face;
L = wall width;
R_d = reduction factor;
R_{inter} = interface strength;
z = depth below the top of the wall;
δ = interface frictional angle;
ϕ' = effective frictional angle;
γ = unit weight;
ν = Poisson's ratio;
σ_x = lateral earth pressure.

REFERENCES

Blight, G. E. (1986). "Pressure exerted by materials stored in silos, Part I: coarse materials." *Geotechnique*, 36(1), 33−46.

Elias, V., Christopher, B. R., and Berg, R. R. (2001). "Mechanically stabilized earth walls and reinforced soil slopes design and construction guidelines." Report No. FHWA-NHI-00-043, National Highway Institute, Federal Highway Administration, Washington, D.C.

Filz, G. M. and Duncan, J. M. (1997a). "Vertical shear loads on nonmoving walls, I: Theory." *Journal of Geotechnical and Geoenvironmental Engineering*, ASCE, 123(9), 856−862.

Filz, G. M. and Duncan, J. M. (1997b). "Vertical shear loads on nonmoving walls, II: application." *Journal of Geotechnical and Geoenvironmental Engineering*, ASCE, 123(9), 863−873.

Frydman, S. and Keissar, I. (1987). "Earth pressure on retaining walls near rock faces." *Journal of Geotechnical Engineering*, ASCE, 113(6), 586−599.

Handy, R. L. (1985). "The arc in soil arching." *Journal of Geotechnical Engineering*, ASCE, 111(3), 302−318.

Hatami, K. and Bathurst, R. J. (2005). "Development and verification of a numerical model for the analysis of geosynthetic reinforced-soil segmental walls." *Canadian Geotechnical Journal*, 42(4), 1066−1085.

Janssen, H. A. (1895). "Versuche uber getreidedruck in silozellen." Zeitschr. d. Verein Deutscher Ingenieure, 1045−1049. (partial English translation in *Proceedings of the Institute of Civil Engineers*, London, England, 1986.)

Jarrett, N. D., Brown, C. J., and Moore, D. B. (1995). "Pressure measurements in a rectangular silo." *Geotechnique*, 45(3), 95−104.

Lawson, C. R. and Yee, T. W. (2005). "Reinforced soil retaining walls with constrained reinforced fill zones." *Proceedings of the Geo-Frontiers 2005*, ASCE, Geo-Institute Conference, 2721−2734.

Leshchinsky, D., Hu, Y., and Han, J. (2003). "Limited reinforced space in segmental retaining walls." *Geotextiles and Geomembranes*, 22(6), 543−553.

Plaxis (2005). *Plaxis Finite Element Code for Soil and Rock Analyses*, Version 8.2, P.O. Box 572, 2600 AN Delft, Netherlands.

Spangler, M. G. and Handy, R. L. (1984). *Soil Engineering*. Harper and Row, New York.

Sperl, M. (2006). "Experiments on corn pressure in silo cells - translation and comment of Janssen's paper from 1895." *Granular Matter*, 8(2), 59−65.

Take, W. A. and Valsangkar, A. J. (2001). "Earth pressures on unyielding retaining walls of narrow backfill width." *Canadian Geotechnical Journal*, 38, 1220−1230.

Woodruff, R. (2003). "Centrifuge modeling of MSE-shoring composite walls." Master Thesis, Department of Civil Engineering, the University of Colorado, Boulder.